

Stability Analysis of the Floating Multi-robot Coordinated Towing System Based on Ship Stability

Dongna Li, Xiangtang Zhao, Zhigang Zhao, Cheng Su, Jiadong Meng

Abstract—Currently, cranes used at sea are insufficient in efficiency. Accordingly, a floating multi-robot coordinated towing system is proposed to meet offshore towing needs. However, the towing robot is prone to overturning because of the system's utilization of rope-driven robot flexibility and its floating attributes in fluid environments. First, the kinematics and dynamics of the towing system are analyzed through coordinate transformations and hydrodynamic theory. Subsequently, physical modeling of the towing system is conducted, with an emphasis on analyzing the system's fluid–structure coupling properties, supplemented by illustrative examples. Finally, the stability of the floating robot is assessed based on ship stability theory, encompassing analyses of the rope tension effects, size and shape of the floating base, and external environmental factors influencing system stability. Results show that the special shape of the floating base is beneficial in reducing water resistance and improving the stability of the floating robot in the flow field. The results provide a good basis for the system structural design and application.

Index Terms—offshore towing, kinematics, dynamics, fluid–structure coupling, ship stability, stability

I. INTRODUCTION

WITH the sharp rise in human demand for energy, particularly the increasing need for marine energy extraction, the demand for offshore platform cranes is also growing. However, individual marine cranes have limitations in terms of their load capacity, efficiency, and safety, rendering them inadequate for heavy cargo operations, replenishment activities at sea, and deep-sea engineering tasks. Accordingly, a novel floating multi-robot towing system emerges by integrating marine cranes into a multi-robot coordinated system. This innovative approach

effectively mitigates the limitations inherent in individual marine cranes, thereby enhancing the efficiency, stability, and safety of towing operations.

The multi-robot coordinated towing system has huge potential for future research [1], the towing robot can be aerial drones [2], [3] or robots fixed on the ground [4], [5]. However, few studies have been conducted on offshore towing. If the single towing robot is fixed on the floating base to form the floating robot, then multiple floating robots in the sea coordinate tow suspended objects. The towing system operates within a fluid environment, where unstable fluid loading and wave actions on the floating robot can significantly influence the safety of the entire operation. Furthermore, the external force at the end of the robot, which may cause the floating robot to overturn. Such overturning during towing can result in the loss of control of the system with no possibility of recovery.

The force of the towing system is related not only to the system itself but also to the motion in the flow field. Specifically, the movement of the floating robot affects the fluid forces acting upon it. The reaction force from the fluid alters the motion of the floating robot. The motion of a floating robot under a wave load is a complex dynamic problem. When the motion of the floating robot is small, the effect of its motion on the flow field can be neglected. However, if the motion significantly affects the flow field, then it necessitates consideration as a bidirectional fluid–structure coupling [6]. In deep-water numerical simulation, results derived from analyzing the quasi-static model often exhibit significant errors. Consequently, the utilization of numerical methods that incorporate fluid–structure coupling becomes essential for resolving the dynamic model under nonlinear forces. Investigation of the fluid–structure coupling of floating robots and fluid loads is the foundation for stability studies. Precise prediction of the impact of waves and currents on a floating robot is instrumental in guiding structural design and stability analysis of the towing system.

Computational fluid dynamics (CFD) has been extensively utilized in flow field calculations, offering valuable insights for theoretical research and practical applications. Horoub et al. [7] studied the influence of rope distribution on the working space of the rope-driven offshore platform. Chandrasekaran et al. [8] simulated the waves, and calculated the wave force of the offshore platform. Lee et al. [9] analyzed the dynamic response of floating cranes using multi-dynamic theory. Katrin et al. [10] developed a 4 degrees of freedom (DOF) dynamical model of the towing

Manuscript received October 6, 2023; revised April 30, 2024.

This work was supported by the Key Research and Development Project of Lanzhou Jiaotong University (Grant No. LZJTU-ZDYF2302).

Dongna Li is an associate professor at the School of Mechanical Engineering at Lanzhou Jiaotong University, Lanzhou 730070, China (e-mail: lidongna@mail.lzjtu.cn)

Xiangtang Zhao is a PhD graduate from Lanzhou Jiaotong University, Lanzhou 730070, China (e-mail: 13220035@stu.lzjtu.edu.cn).

Zhigang Zhao is a professor at the School of Mechanical Engineering at Lanzhou Jiaotong University, Lanzhou 730070, China (corresponding author to provide phone: 0931-4956047; fax: 0931-4938023; e-mail: zhaozhg@mail.lzjtu.cn).

Cheng Su is an associate professor at the School of Mechanical Engineering at Lanzhou Jiaotong University, Lanzhou 730070, China. (e-mail: sucheng@mail.lzjtu.cn).

Jiadong Meng is an associate professor at the School of Mechanical Engineering at Lanzhou Jiaotong University, Lanzhou 730070, China (e-mail: mengjiadong@foxmail.com).

ship and performed time and frequency domain analysis of the system using numerical calculation methods. They further validated the model through ship mode experiments, ensuring its accuracy and reliability. Dong et al. [11], [12] used the principle of vector mechanics to explore the displacement of the suspended object and the rope tension in the wave. Zhu et al. [13], [14] studied the floating crane system composed of a double crane ship and analyzed the impact of wave and towing speed on the shaking of the suspended object. Existing studies only examine the effect of the towing platform on the suspended object, but not its motion and stability in the wave. Wang et al. [15] analyzed the effect of fluid–structure coupling on the wave force of a single pile. Gu et al. [16] studied the fluid–structure coupling response of the platform under random waves and solved the motion of the time domain by using the Runge–Kutta method. Zhang et al. [17] investigated the fluid–structure coupling of floating platforms and examined the significant influence of this factor on the motion of the floating platform. The analyses conducted by scholars across the world indicated that when the motion of the floating platform is significant, the fluid’s reaction force alters the wave force. A viable solution to address this involves simplifying the floating platform to a beam cell model. Researchers can investigate the genuine dynamic response of the floating crane in the designed pool by utilizing this reduced model.

The stability of floating towing ships and floating platforms has been intensively studied by scholars worldwide. Ding et al. [18] calculated the complete stability and broken stability of the offshore floating tank using finite element software. Liu [19] analyzed the principle of roll stability by using the motion equation of ships. Zhang et al. [20] adopted the stochastic function and phase space transmission theory to study the overturning process of ships and established the equation of the ship rolling. Sun et al. [21] adapted the stability criterion of the submarine and studied the motion stability of the vertical surface of the AUV. The analyses conducted by the above-mentioned scholars indicated that stability analysis of a ship typically involves utilizing the Archimedean principle to determine specific parameters, such as the center of gravity and buoyancy. Stability analysis involves calculating the correlation between the tilt angle and the restoring moment of the ship under various operational conditions. During calculations, the ship is presumed to gradually tilt when external forces are incrementally applied. The stability theory of the ships can be used to analyze the stability of the system.

The towing system, utilizing multiple ropes to tow an object within a fluid environment, represents an unconstrained system highly susceptible to external disturbances. Conducting stability experiments with actual objects poses significant risks, emphasizing the importance of theoretical and simulation analyses to assess the stability of the towing system. The outline of the paper is organized as follows. In Section II, the spatial configuration of the towing system is described, and the kinematic model is established using the coordinate transformation method. In Section III, the dynamic models for the parallel towing system and the floating robot are developed based on rigid-body and fluid dynamics, respectively. In Section IV, the stability of the towing system is analyzed by using ship stability theory. In

Section V, the physical modeling is performed based on the spatial configuration of the towing system, and the fluid–structure coupling characteristics of the towing system are analyzed. In Section VI, a stability criterion for the towing system is established, and the factors influencing towing stability are thoroughly analyzed. Finally, Section VII presents the conclusions drawn from the study.

II. KINEMATIC ANALYSIS

A. Structure

The structure of the towing system is shown in Fig. 1, the suspended object is connected to the end of the floating robot via ropes, the floating robot is divided into two parts: the floating base and the joint manipulator. During towing operations, the suspended object follows a predefined trajectory through adjustments in the positions of the floating robot. Additionally, the suspended object’s position can be altered by modifying the length of the rope. The floating base is powered by a propeller to move it. The floating robot is typically equipped with a self-balancing device to effectively eliminate the swaying and pitching of the towing robot, thereby maintaining the system stability.

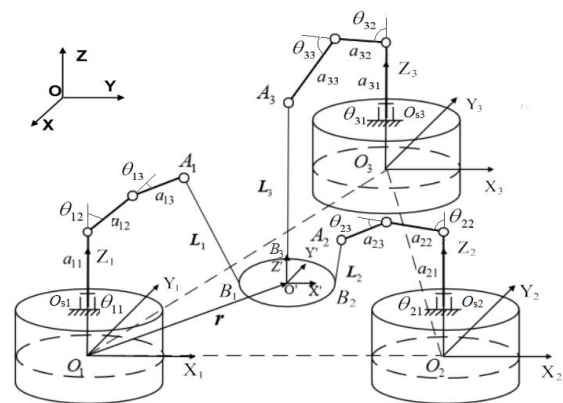


Fig. 1. Structure of the towing system

The coordinate systems $\{O-XYZ\}$, $\{O_i-X_iY_iZ_i\}$, $\{O_{si}-X_{si}Y_{si}Z_{si}\}$, and $\{O'-X'Y'Z'\}$ are established according to the structure of the towing system. Furthermore, the pole length of the robot is (a_{11}, a_{12}, a_{13}) , the angle is $(\theta_{11}, \theta_{12}, \theta_{13})$, and the pose of the suspended object is $(x, y, z, \varphi_1, \varphi_2, \varphi_3)$.

The towing system can be categorized into three types based on the different system drivers: ① Systems where only the rope length changes. ② Systems where only the position of the end of the robot changes. ③ Systems where the length of the rope and the position of the end of the robot simultaneously change. Moreover, systems can be classified according to the number of translational DOF of the suspended object: when the suspended object under study has only three translational DOF, it is called a 3T configuration. When the suspended object under study has 6 DOF, it is called the 3R3T configuration. This work primarily focuses on studying the relevant characteristics of the towing system and will not elaborate on a single robot.

In systems where the number of robots is three or more, the rank of its structural matrix is consistently three. The towing system is studied in this work using three robots with three

translational DOF as an example to enhance the typicality of the subject matter, $i = 1, 2, 3$. The floating robot is considered in its optimal working state.

B. Kinematic Analysis

In the coordinate system $\{O\}$, the motion of the floating base can be expressed as follows:

$$q = (x_s, y_s, z_s, \alpha, \beta, \gamma)^T \quad (1)$$

In coordinate system $\{O_i\}$, the D–H transformation method allows for the direct determination of coordinate $(x_{pi}^*, y_{pi}^*, z_{pi}^*, 1)$ of the towing robot end. Thereafter:

$$\begin{bmatrix} x_{pi}^* \\ y_{pi}^* \\ z_{pi}^* \\ 1 \end{bmatrix} = \begin{bmatrix} a_{i3} \cos \theta_{i1} \cos \theta_{i2} \cos \theta_{i3} - a_{i3} \cos \theta_{i1} \sin \theta_{i2} \sin \theta_{i3} + a_{i2} \cos \theta_{i1} \cos \theta_{i2} \\ a_{i3} \sin \theta_{i1} \cos \theta_{i2} \cos \theta_{i3} - a_{i3} \sin \theta_{i1} \sin \theta_{i2} \sin \theta_{i3} + a_{i2} \sin \theta_{i1} \cos \theta_{i2} \\ a_{i1} + a_{i2} \sin \theta_{i2} + a_{i3} \cos \theta_{i2} \sin \theta_{i3} + a_{i3} \sin \theta_{i2} \cos \theta_{i3} \\ 1 \end{bmatrix} \quad (2)$$

The coordinate of the towing robot end is (x_{pi}, y_{pi}, z_{pi}) in coordinate system $\{O\}$. Subsequently:

$$\begin{bmatrix} x_{pi} \\ y_{pi} \\ z_{pi} \\ 1 \end{bmatrix} = \mathbf{R}^* \mathbf{R} \begin{bmatrix} x_{pi}^* \\ y_{pi}^* \\ z_{pi}^* \\ 1 \end{bmatrix} \quad (3)$$

where \mathbf{R}^* is the transformation matrix between coordinate systems $\{O_i\}$ and $\{O_{si}\}$, and \mathbf{R} is the transformation matrix between coordinate systems $\{O_{si}\}$ and $\{O\}$.

In coordinate system $\{O\}$, we can derive the motion relationship between the end of the towing robot and the floating base by combining Eqs. (1) – (3).

III. DYNAMICAL ANALYSIS

A. Dynamic Analysis of the Floating Robot

The force acting at the end of the towing robot and the internal force of the robot are converted into force and torque on the floating base. The binding and torque on the robot joint must be analyzed because the towing processes may potentially cause overturning of the floating base.

In this section, the Newton–Euler iterative kinetic equation is applied to calculate the force and torque from the robot end to the floating base. Taking joint 1 as an example, the force and torque applied at the robot joint are expressed as follows:

$$\mathbf{M}_1 = \mathbf{M}_{g1} + {}^v\mathbf{M}_{m1} + {}^a\mathbf{M}_{m1} + \mathbf{M}_{f1} \quad (4)$$

where \mathbf{M}_{g1} , ${}^v\mathbf{M}_{m1}$, ${}^a\mathbf{M}_{m1}$, and \mathbf{M}_{f1} represent the binding force and torque caused by the mass of robot links, joint angular velocity, joint angular acceleration, and the rope tension of the robot end. Refer to the literature for the detailed expression.

In the dynamic analysis of the swaying motion of a floating robot under the influence of regular incident waves, the complexity of the actual towing system necessitates certain assumptions. According to the idea [22] of separation modeling, the restraining reaction force and the interaction force in the system are ignored, and the interference force (moment) is attached to the mathematical model of the floating robot motion as an external force. This interference

force can be decomposed into three components: the force exerted by the flow field, the force exerted by the robot, and the tension in the rope.

From a mechanical point of view, the oscillatory motion of a floating robot on a fluid is divided into two main parts: one is the rigid body dynamics problem, the other part is the hydrodynamic problem. Specifically, the 6 DOF motion of the floating robot in the wave should be analyzed. However, the analysis becomes more difficult as the number of DOF increases. The following assumptions are made in the establishment of the dynamic model: the motion of the floating robot in the water can be regarded as the forced vibration of the rigid body, and the 6 DOF motion is independent of each other. The motion on each degree of freedom of the floating robot is separated, and the modeling is discussed separately.

The simplest method involves studying the heave motion of the floating robot and establishing the equation of the floating robot under the combined action of wave force (excitation and radiation forces), hydro-static recovery force, and damping force. The fluid is assumed to move according to the simple harmonic law (Fig. 2(b)). Meanwhile, the floating base is constrained in other directions except the heave direction, and the wave disturbance force of the fluid on the floating base is F_w . The floating base is in an unconstrained state and does heave motion under the action of wave disturbance force F_w (Fig. 2(c)). Z is the displacement, F_r is the vertical restoring force, F_d is the damping force, and F_a is the inertial resistance.

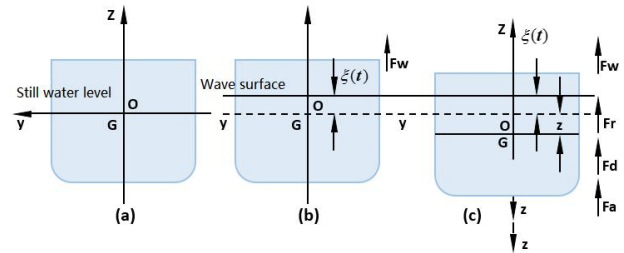


Fig. 2. Diagram of the floating base

The motion equation of the floating robot in the heave direction is expressed as follows:

$$\mathbf{M}_z z'' + 2\mathbf{N}_z z' + \mathbf{C}_z z = \mathbf{F}_z + \mathbf{T}_z \quad (5)$$

where $\mathbf{M}_z = m + \lambda_z$; $\mathbf{C}_z = \rho S_w$; m is the floating robot mass; λ_z is the additional mass coefficient; z'' is the acceleration; ρ is the density of water; S_w is the waterline surface area; \mathbf{N}_z is the damping coefficient; and \mathbf{F}_z and \mathbf{T}_z denote the wave disturbance force and the rope tension, respectively.

The differential equations on the remaining DOF can be established according to the above-mentioned assumptions and methods:

$$\begin{cases} \mathbf{M}_x x'' + 2\mathbf{N}_x x' + \mathbf{C}_x x = \mathbf{F}_x + \mathbf{T}_x \\ \mathbf{M}_y y'' + 2\mathbf{N}_y y' + \mathbf{C}_y y = \mathbf{F}_y + \mathbf{T}_y \\ \mathbf{M}_\alpha \alpha'' + 2\mathbf{N}_\alpha \alpha' + \mathbf{C}_\alpha \alpha = \mathbf{F}_\alpha + \mathbf{M}_\alpha \\ \mathbf{M}_\beta \beta'' + 2\mathbf{N}_\beta \beta' + \mathbf{C}_\beta \beta = \mathbf{F}_\beta + \mathbf{M}_\beta \\ \mathbf{M}_\gamma \gamma'' + 2\mathbf{N}_\gamma \gamma' + \mathbf{C}_\gamma \gamma = \mathbf{F}_\gamma + \mathbf{M}_\gamma \end{cases} \quad (6)$$

where M , N , C , F , and T (M) are the inertial force, damping force, recovery force, wave disturbance force, and rope force

(torque) coefficient, respectively; and their subscripts represent the respective degree of freedom.

Taking the heave direction dynamic model as an example, the method for determining the coefficients in the second-order differential motion equation of the floating robot under various working conditions is provided.

The additional mass of the heave motion is of the same order of magnitude as the mass of the floating robot; thus, it can be approximated as follows:

$$\lambda_{zz} = D/g \quad (7)$$

The displacement of the floating robot is calculated as follows:

$$D = \gamma V = \gamma C_B LBE \quad (8)$$

where L , B , E , and CB represent the length, width, draft, and square coefficient, respectively, which are the fixed structural parameters of the floating robot.

The load waterline area is expressed as follows:

$$S_w = C_w LB \quad (9)$$

where the water surface line coefficient C_w belongs to the fixed structural parameter of the floating robot.

The damping coefficient of heave motion can be roughly estimated by using the Bubroff formula:

$$2N_{zz} = fS_w \quad (10)$$

where the estimated value in the formula is $f=0.18$.

The damping coefficient and the additional mass coefficient in the second-order differential equation for a floating robot can be calculated in various ways. A relatively simple calculation is chosen in this manuscript to simplify the model. Meanwhile, the detailed coefficient calculations can be performed using slice theory. The Froude–Krylov hypothesis is utilized to compute the disturbing force of the waves, thus yielding the following expression for the disturbing force of waves:

$$F_w = \rho g a k e^{-k \frac{d}{2}} (Bd) \frac{\sin\left(k \frac{BL}{2} \sin \phi\right)}{k \frac{BL}{2} \sin \phi} \int_{-\frac{L}{2}}^{\frac{L}{2}} \cos(kx \cos \phi - \omega_e t) dx \quad (11)$$

where $\omega_e = \left| \omega + \omega^2 v \cos \phi / g \right|$ is the encounter frequency, ϕ is the direction angle of the wave, v is the sailing speed of the floating robot, and ω is the wave frequency.

B. Dynamic Analysis of the Towing System

The suspended object may swing due to the inertial force, disrupting the dynamic balance. Even in the absence of external disturbances, the suspended object will inevitably swing when the robot adjusts its joint angle. Accordingly, the dynamics of the towing system must be established, and the forces on the suspended object must be analyzed. Fig. 3 shows the structural diagram of the towing system, where H denotes the end point of the towing robot, E represents the load, d is the cable length, m_o is the load mass, and the cable force is T .

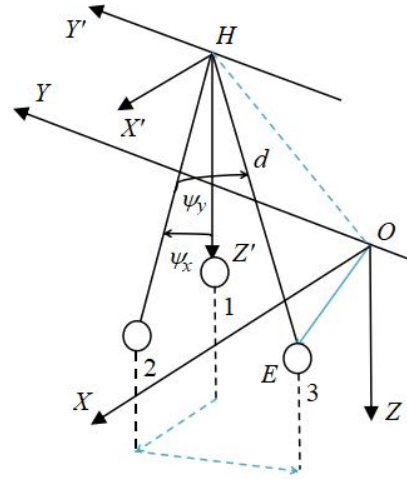


Fig. 3. Diagram of the suspended object

Assuming that the cable is parallel to the Z -axis in the initial state, the cable rotates a degree ψ_x during the load movement from state 1 to state 2. When the load moves from state 2 to state 3, the cable rotates a degree ψ_y . Accordingly, the position of the load is denoted as follows:

$$\begin{cases} x_e = x_h + d \cdot \sin \psi_x \cos \psi_y \\ y_e = y_h - d \cdot \sin \psi_y \\ z_e = z_h + d \cdot \cos \psi_x \cos \psi_y \end{cases} \quad (12)$$

The dynamic equation of the load is expressed as follows:

$$\begin{cases} m_o x_e'' = -T \sin \psi_x \cos \psi_y \\ m_o y_e'' = T \sin \psi_x \sin \psi_y \\ m_o z_e'' = T \cos \psi_x - m_o g \end{cases} \quad (13)$$

The cable tension is obtained by Eq. (13).

$$\begin{aligned} T = m_o g \cos \psi_x + m_o d \cdot [\psi_x'^2 + \sin^2 \psi_x \cdot \psi_y'^2] \\ - m_o x_e'' \sin \psi_x \cos \psi_y + m_o y_e'' \sin \psi_x \cdot \sin \psi_y \\ + m_o z_e'' \cos \psi_x - m_o d \end{aligned} \quad (14)$$

IV. SHIP STABILITY THEORY

Existing studies typically only consider the impact of the towing platform on the suspended object. However, the impact of the suspended object on the towing platform is rarely studied, and the motion law and stability of the towing platform in waves are not considered. A floating robot, a unique type of floating body, is susceptible to overturning during an operation due to the combined effects of fluid forces and rope tension. Therefore, the stability of the floating robot must be studied to ensure stable support without tipping.

Moreover, the stability of the ship includes small inclination stability and large inclination stability. Small-dip stability means that the ship tilts at a small angle and returns to its equilibrium position by a couple of gravity and buoyancy. With regard to the inclination of a large inclination angle, the calculation method of a small inclination angle will have a large error. Accordingly, when analyzing the stability for larger inclination angles, external forces are typically applied to the hull, and that the hull slowly tilts. Stability is then assessed based on the relationship between the hull's inclination angle and the restoring moment under various

operating conditions.

Given that the longitudinal size of a regular ship far exceeds the transverse size, the transverse motion increases the wave force on the ship, and a large transverse motion can even cause the ship to capsize. Only the lateral stability of the ship is considered for simplicity. The stability curve of a floating robot in static water is established based on the stability measure of ships, and the influence of waves, suspended objects, and floating base on the stability of the towing system is analyzed.

The cross-section of the floating base is examined to elucidate the stability principles of the floating robot, in accordance with the above-mentioned requirements (Fig. 4). The floating base is floating on the waterline W_0L_0 in the initial moment, the inclined waterline is $W_\alpha L_\alpha$ when the heeling angle of the floating base is α , and NN' is the reference axis of the calculated static moment.

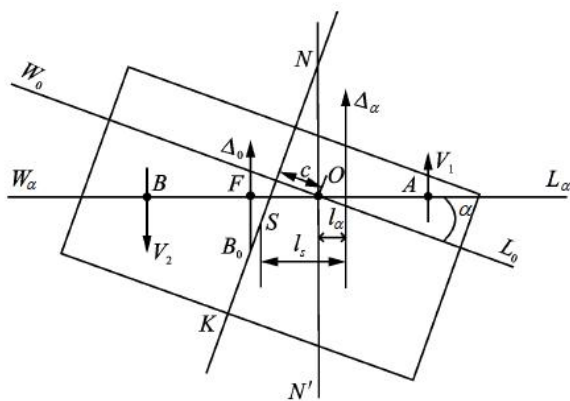


Fig. 4. Schematic of the floating base tilt

The drainage volume Δ_α below the water line $W_\alpha L_\alpha$ is expressed as follows:

$$\Delta_\alpha = \Delta_0 + V_1 - V_2 \quad (15)$$

where Δ_0 is the drainage volume, V_1 is the volume of the water wedge, and V_2 is the volume of the water wedge.

According to the principle of the resultant moment, Fig. 4 demonstrates that the volume static moment of Δ_α with respect to NN' is expressed as follows:

$$M_\alpha = V_1 l_1 + V_2 l_2 - \Delta_0 l_0 \quad (16)$$

where l_1 is the distance from intersection point A to rotation point O of the gravity action line of the water inlet wedge V_1 and the inclined waterline $W_\alpha L_\alpha$, l_2 is the distance from intersection point B of the buoyancy action line of the outlet wedge V_2 and the inclined waterline $W_\alpha L_\alpha$ to the rotation point O, l_0 is the distance from the intersection F of the original drainage volume Δ_0 buoyancy action line and the inclined waterline $W_\alpha L_\alpha$ to rotation point O.

Equation (16) demonstrates that when the floating base floats on the inclined waterline $W_\alpha L_\alpha$, the distance between the buoyancy action line and the axis NN' is expressed as follows:

$$l_\alpha = \frac{M_\alpha}{\Delta_\alpha} = \frac{V_1 l_1 + V_2 l_2 - \Delta_0 l_0}{\Delta_0 + V_1 - V_2} \quad (17)$$

The value of l_0 (Fig. 4) is obtained as follows:

$$l_0 = (d_0 - d_{KB_0}) \sin \alpha + c \cos \alpha \quad (18)$$

$$V_1 l_1 + V_2 l_2 = \frac{1}{3} \int_{-\frac{L}{2}}^{\frac{L}{2}} \int_0^\alpha (a^3 + b^3) \cos(\alpha - x) d\alpha dx \quad (19)$$

where d_0 is the depth of draft, d_{KB_0} is the distance between the center of buoyancy B_0 and midpoint K at the bottom of the cross-section of the floating base, c is the deviation value, and L is the length of the floating base. The water inlet and outlet wedges are divided into infinite small wedges, and a small triangle with an angle of $d\alpha$ is taken at α , and the distance between the bottom edge is a and b , respectively.

l_α can be obtained by substituting Eq. (19) into Eq. (17), and the horizontal distance between the line of buoyancy and the line of gravity is obtained.

$$l_s = l_\alpha + (d_0 - l_3) \sin \alpha + c \cos \alpha \quad (20)$$

where l_3 is the distance between midpoint K at the bottom of the cross-section of the floating base and the assumed center of gravity S of the floating base when it is floating.

With the floating robot in a certain incline range, the restoring moment ensures that the floating robot does not tip over after repeated pitches. Eventually, equilibrium is attained due to the combined effects of resilience and damping forces. However, a critical inclining angle exists, beyond which the overturning of the floating robot becomes irreversible. At this critical point, when the dynamic transverse torque reaches the minimum overturning torque, the transverse torque and the restoring moment exert equal influence, enabling the floating robot to maintain its balance.

The above analysis indicates that the stability of the floating robot is contingent upon the restoring moment, which is the product of displacement and the righting arm. Under the same displacement, the righting arm directly reflects the stability of the floating robot. Accordingly, maximization of the righting arm is crucial to enhance the stability of the floating robot. A method for calculating the transverse righting arm is introduced, assuming that the external force is gradually added to the floating robot, the floating robot slowly tilts, only the transverse component of the righting arm is calculated in the cross-section, and the longitudinal component of the righting arm is ignored, to approximate the equivalent total righting arm [23]. This approximate computational method has been demonstrated to uphold the safety and reliability standards observed in a wide array of real ships.

V. ANALYSIS OF FLUID-STRUCTURE COUPLING

The motion of an offshore platform under wave load is a complicated dynamic problem. If the platform's motion significantly affects the flow field, then it necessitates consideration as a fluid-structure coupling problem to effectively address it.

The motion of the floating robot disrupts the surrounding fluid, altering the velocity and pressure distribution of the fluid around the robot. When the wave passes through the

floating robot, the fluctuation of the wave changes the contact area between the floating robot and the fluid and makes the buoyancy change. A bidirectional fluid–structure coupling analysis is one in which the results of the fluid and structure are transferred through the coupling plane when the structural response is large. Considering the interaction between the flow field and the floating robot, the floating robot in the flow field will be subjected to fluid force, and the motion of the floating robot also affects the fluid force. The floating multi-robot coordinated towing system has typical two-way fluid–structure coupling characteristics. When fluid flows around the floating robot, alternating pressure differences occur at its upper and lower boundaries, resulting in significant vibration and potential overturning of the floating robot. Research on the fluid–structure coupling between the floating base and the fluid load serves as the foundation for investigating its stability.

Under the influence of waves, a strong coupling relationship exists between the rigid bodies (such as the floating robot and suspended object) and the flexible body (the rope), as well as the fluid surrounding the system. During the towing process, the rope tension changes, thereby affecting the buoyancy of the base. Changes in the buoyancy of the base induce shaking in the floating robot, while the swaying motion of the floating robot imparts forces on the surrounding fluid, resulting in alterations in the flow field. Consequently, the stress conditions and motion responses of the floating robot are affected. In the fluid–structure coupling analysis, the working environment of the towing system is the complex wave environment, wherein only the excitation from fluid and wave forces acting on the floating robot are considered. The 3D model established according to the design requirements and dimensions is shown in Fig. 5.

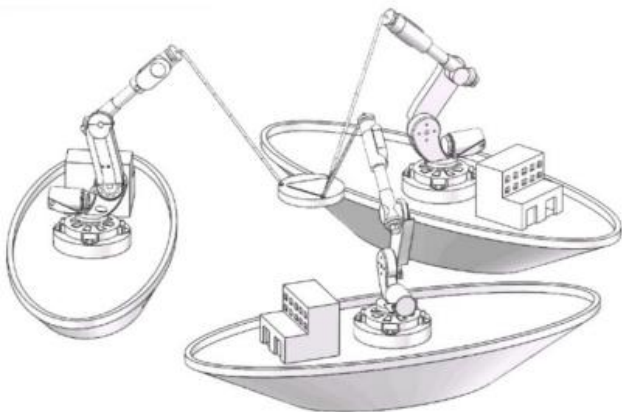


Fig. 5. Model of the floating multi-robot towing system

A. Modeling of Fluid–Structure Coupling

In hydrodynamic analysis, the specific steps are pre-processing, numerical iterative solution, and simulation post-processing. The fluid–structure coupling model of the towing system includes the fluid and solid models. The pre-processing typically includes the following steps:

(1) The establishment of a finite element model involves treating the robot joint angle as fixed under vertical towing conditions, with the robot and floating base treated as a single rigid body. The end position of the towing robot is fixed, and the suspended object is towed to the specified position by

changing the rope length.

(2) The establishment of a computational domain model involves creating and dividing the computational domain surrounding the model into tetrahedral meshes. The size of the guaranteed cube area does not adversely affect the analysis of the towing system model, and the edge length of the given cube area is 80 m.

(3) The computing grid is divided, and the properties of the fluid are determined. The grids are divided using Gambit software, the unstructured grids are used to divide it, and the grids at the connection between the robot and the floating base are encrypted.

(4) Determination of the boundary conditions and configuration of the calculation parameters involve specifying the following: The inlet of the chosen fluid domain is the velocity inlet, the surface of the floating robot is the non-slip surface, the domain wall is the calculated symmetric boundary, and the outlet of the fluid domain is the pressure outlet. The grid of the fluid domain is configured in the dynamic grid mode, enabling movement of the fluid–structure coupling boundary and sub-fluid domain. The fluid attribute is selected as in-compressible, and the simulation condition is the 3D pressure-based model, solving the equation to select the $k-\xi$ model.

(5) The output parameters are set, and the analysis type and load step are determined.

B. Solving of Fluid–Structure Coupling

Fluent software provides a dedicated mode of fluid–structure coupling analysis. After the fluid and solid regions are assigned, the software automatically identifies the fluid–structure coupled boundaries, sets the boundary loads, and moves the grid without manual programming. The solution principle is as follows: in the fluid domain, the fluid force on the solid is solved; in the solid domain, the displacement transmitted to the fluid is obtained [24]. Specifically, the pressure in the fluid equation is solved over a time step. Subsequently, this pressure is applied as a boundary load to the solid domain's boundary to ascertain the solid's displacement. This displacement guides the deformation of the dynamic mesh, and the updated mesh is utilized to compute the fluid pressure for the subsequent time step. The load and displacement are transferred at every moment by setting the solver, coupling surface conditions, and parameter initialization.

The motion range of the floating robot in extreme conditions may be significant, rendering frequency domain analysis inadequate for accurately depicting real-time motion. Accordingly, time-domain analysis is adopted to solve the problem, the first stage is 0–40 s, wherein the three ropes shrink at a 0.5 m/s speed; the second stage is 40–120 s, wherein the towing system enters the self-balance stage. During the fluid–structure coupling analysis, the simulated time $T = 120$ s is divided into 12,000 time-steps, and each time step is $\Delta T = 0.01$ s.

The divided grid model is introduced into Fluent software, after determining the corresponding boundary constraints, analysis type, analysis options, and load steps, and the corresponding results can be obtained. The parameters in the

solving process are set according to the actual towing conditions. The post-processing process puts the results through the curve or list.

C. Example Simulation

The size and configuration of the floating base exert significant influence on the stability of the system, serving as a foundational element for the stability analysis of the floating robot. Before studying the stability of the floating robot, the relationship between the shape of the floating base and the fluid force should be known. The towing system, a new type of water towing equipment, has no professionally designed specifications to refer to. The work proposes three different shapes of the floating base (Fig. 6), and the surface of various sections has the same height. This work investigates the effect of wave conditions on the stability with multiple floating bases of different section shapes. thereby furnishing critical insights for the stability analysis.

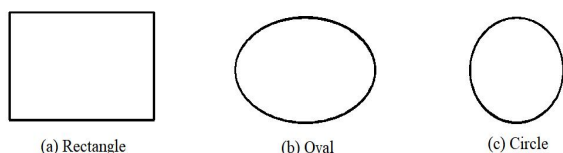


Fig. 6. Different cross-sections of the floating base

The fluid analysis module Fluent within ANSYS served as the simulation platform for this study. The multi-phase flow model in Fluent is utilized to simulate wave generation. This approach facilitated the observation of the liquid flow process. The 6 DOF model is used to simulate the motion of the floating robot, and user defined functions is utilized to control the number of DOFs of the floating robot. The function can simulate a variety of working conditions.

The initial parameters of the floating robot are set, where the structure of the floating base is an ideal ellipse with a long half-axis of 4 m, a short half-axis of 3 m, and a height of 4 m. When the floating robot is stationary on the water surface, the draft depth of the floating base is 2 m, the water consumption is $4.0 \times 10^3 \text{ kg}$, and the fluid density is $\rho = 10^3 \text{ kg/m}^3$. The three floating robots are arranged in a triangular shape. The initial positions of the barycenter and end of the three floating robots are shown in Table I.

	X(m)	Y(m)	Z(m)
O_{s1}	0	35	0
O_{s2}	$-17.5\sqrt{3}$	-17.5	0
O_{s3}	$17.5\sqrt{3}$	-17.5	0
p_1	0	20	30
p_2	$-10\sqrt{3}$	-10	30
p_3	$10\sqrt{3}$	-10	30

Initially, the object is suspended in the air, maintaining a state of static equilibrium. This work presumed that the position of the suspended object barycenter before towing is (0, 0, 0), and that of the barycenter after towing is (0, 0, 10). The parameters of the system are shown in Table II.

TABLE II
PARAMETERS OF THE TOWING SYSTEM

Parameter	Symbol	Value
Mass of suspended object	m_o	$1.6 \times 10^3 \text{ kg}$
Mass of base	M	$3.2 \times 10^3 \text{ kg}$
Length of the rope	L_i	30 m
Size of link 1	a_1	10 m
Size of link 2	a_2	15 m
Size of link 3	a_3	15 m
Mass of link 1	m_1	$8.76 \times 10^2 \text{ kg}$
Mass of link 2	m_2	$1.314 \times 10^3 \text{ kg}$
Mass of link 3	m_3	$1.314 \times 10^3 \text{ kg}$

Taking the elliptical base of the floating robot as an example, the wave height and wavelength of the fluid are determined by the multi-phase flow setting in Fluent. Under the wave condition, the three-level sea condition is selected as the towing condition of the towing system, the wave speed is 1 m/s, wave height is 1 m, the wavelength is 10 m, the wave angle is zero, the water depth is 40 m, and the flow direction is along the X-axis.

One of the three floating robots is used as an analytical example due to the symmetric configuration of the towing system. When subjected to wave action, integration of the linear fluid pressure across the surface of the floating base enables the determination of buoyancy and restoring moments of the floating robot. The average of the buoyancy and restoring moment is taken as the simulation value under the towing condition [25]. Only a representative response curve is extracted for clarity in examining the time-domain response. The simulated results are shown in Figs. 7 and 8.

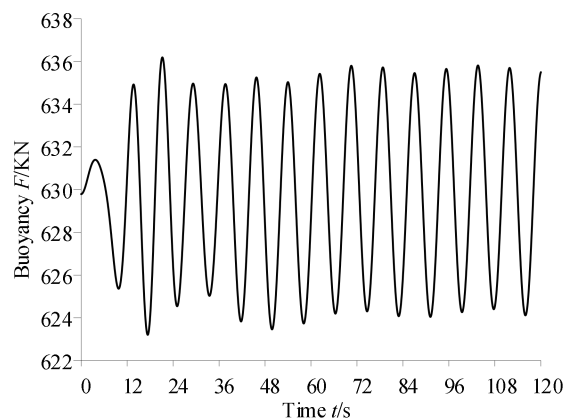


Fig. 7. Buoyancy curve

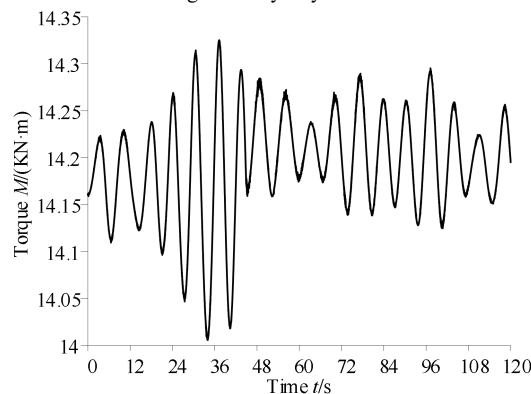


Fig. 8. Restoring moment curve

The buoyancy of the floating robot exhibits minor

fluctuations under the combined influence of hydrodynamics and rope tension (Fig. 7 and 8). The floating base sinks more, and the resilience torque of the floating robot sharply increases due to the influence of wave load on the towing system. When the rope stops contracting, the energy in the towing system cancels out, and the buoyancy and restoring moment curves are more stable. Consequently, the towing system sustains operation without failure despite ongoing wave action.

The following conclusions are drawn by analyzing the buoyancy and restoring moments of a rectangular base and a cylindrical base floating robot. Under the condition of equal inflow surface area, the blunt body cross-section with a complex shape will result in greater viscous drag. By contrast, a smoothly curved shape of the floating base can reduce the surface pressure of the floating robot, thereby improving stability. Therefore, the section shape with edges and corners should be avoided in the design of the floating robot, the floating base is streamlined to reduce the pressure drag, and the shape of the floating base is finally determined to be a cylinder.

VI. STABILITY ANALYSIS

A. Stability Criteria

The stability of a system can be classified into three aspects: motion state, structure, and form. In terms of motion state, stability can be categorized as static stability and dynamic stability. In terms of system structure, stability can be classified as the stability of the suspended object and the stability of the floating robot. In terms of form, stability can be divided into structural stability and control stability. This work focuses on the analysis of the stability of the floating robot.

When a floating robot is stationary on a fluid surface, it is in an equilibrium state. However, during the process of towing an object, the floating robot is subjected to external forces, such as tension in the ropes and fluid forces, which disturb its balance and cause it to tilt. Questions arise regarding whether the floating robot will overturn under these external forces, and whether it will return to its initial position once the external forces cease. This situation relates to the stability of the towing system. The static stability of the floating robot is analyzed based on the stability criteria of the ship.

During the operation of a floating robot, rope tension and fluid forces on the floating robot may cause the entire towing system to overturn. When discussing the stability of a floating robot, the position of the inclining waterline and the center and magnitude of buoyancy must be determined, and the size and direction of the restoring moment must be analyzed. Finally, the relationship between the transverse angle and the righting arm is studied to measure the stability, namely, the stability curve. In the stability evaluation of the towing system, the maximum right arm of the floating robot should not be less than 0.2 m, and the corresponding inclined angle should not be less than 15. The steps are as follows:

- (1) When the floating robot tilts, the position of the inclined waterline is determined.
- (2) The displacement, buoyancy, and buoyant center position are obtained under the inclined waterline.

(3) The restoring moment and inclined torque are calculated according to the actual conditions.

(4) Starting from the positive floating position of the floating robot, the inclined angle of the floating robot is divided from 0 to 40. In each tilt angle, the righting arm is calculated based on the restoring moment. The calculated data points are then connected by lines to form a static stability curve of the floating robot.

The static stability curve is just a schematic, and the floating robot is in static balance at each inclined angle. The floating robot remains in a stable state until it reaches the critical inclined angle, beyond which it is prone to overturning.

B. Factors Affecting the Towing Stability

The factors that affect the stability of the floating robot are analyzed based on the stability criteria of the ship. Meanwhile, the factors that influence the stability are categorized into internal and external elements. External factors encompass the presence of the suspended object attached to the towing robot and environmental conditions encountered during towing operations. The internal factors lie in the properties of the system itself (the gravity of the robot, the size and shape of the floating base, etc.). The floating robot is placed in the flow field at different transverse inclined angles to verify the correctness of the stability method. The stability of the towing system can be comprehensively analyzed across diverse scenarios by plotting the righting arm curve for the floating robot under these conditions.

The stability curve of the floating robot when towing different loads using the static method is shown in Fig. 9, and the influence of the load on the stability of the towing system is analyzed. Fig. 10 showcases the stability curves of the floating robot under static water conditions and during peak and trough wave states. The stability curves of the floating robot at different wavelengths are shown in Fig. 11. The floating base of three different shapes is proposed to study the stability along with the shape and size of the floating base (Figs. 12–14).

Impact of the suspended object

When the floating robot tilts at a small angle, the pose change of the suspended object can be seen as adding an external torque to the floating robot. Accordingly, the restoring moment will decrease, and the stability of the floating robot will decrease. The maximum inclined angle of the floating robot decreases when the mass of the suspended object increases, and the maximum value of the righting arm significantly decreases (Fig. 9). This phenomenon indicates that the towing system's capacity to withstand external torque is gradually diminishing. When the mass of the suspended object is 30 t, the maximum righting arm corresponding to the inclined angle is less than 15, indicating that the towing system will overturn under the condition.

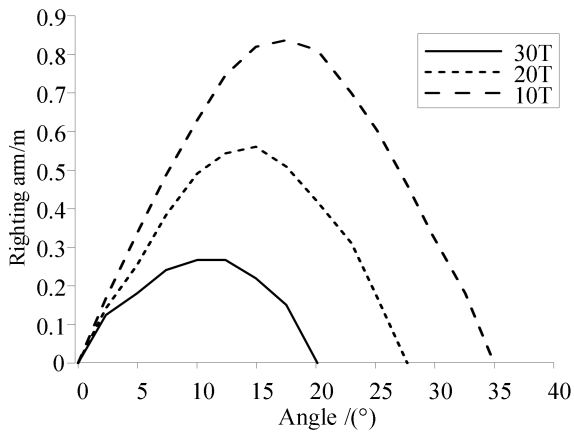


Fig. 9. Stability curves under different loads

Impact of the waves

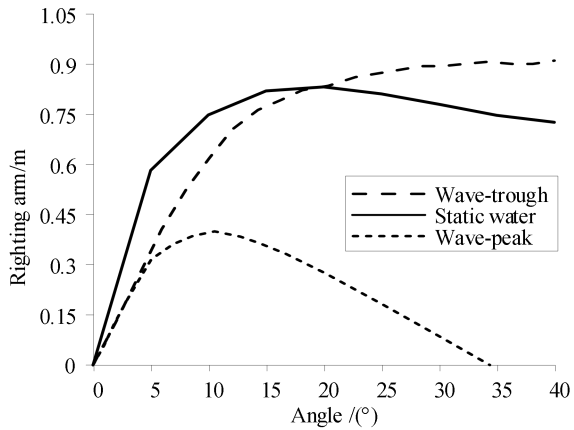


Fig. 10. Stability curves at different wave conditions

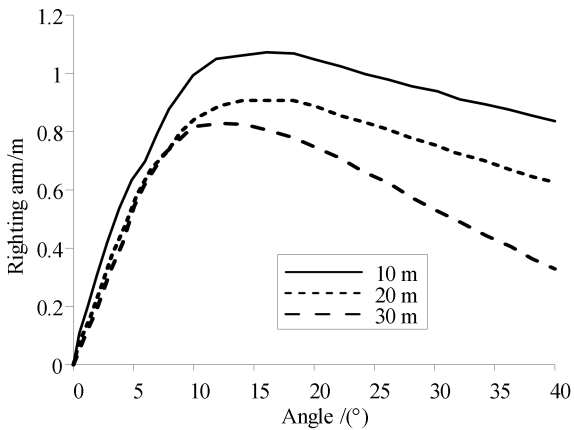


Fig. 11. Stability curves at different wavelengths

In the wave environment, Fig. 10 shows that the righting arm of the floating robot experiences a considerable reduction at the wave peak compared with the wave trough and static water conditions, accompanied by a corresponding decrease in the finite inclined angle. When other conditions are the same, the floating robot is on the wave peak for a long time, and it will overturn due to the insufficient restoring moment. The wavelength has different effects on the stability of the towing system (Fig. 11). Specifically, longer wavelengths result in greater righting arms, thereby enhancing the overall stability of the towing system. When the wavelength is 10 m, the maximum righting arm corresponding to the inclined angle is not greater than 15, and the towing system will overturn. Considering the

above-mentioned results, when the operator performs the towing task in the wave, the towing robot of the towing system should be avoided in the wave peak and short wavelength.

Impact of the floating base

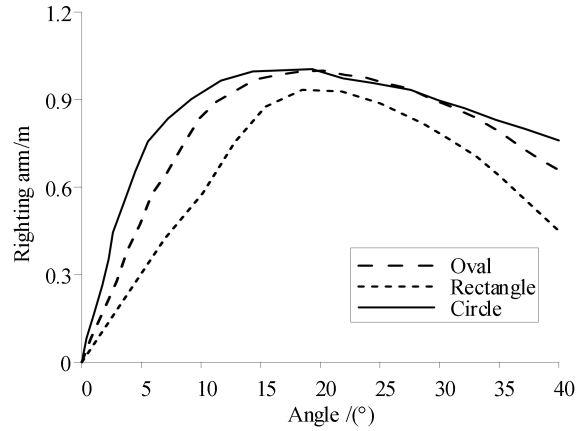


Fig. 12. Stability curves for the different shapes

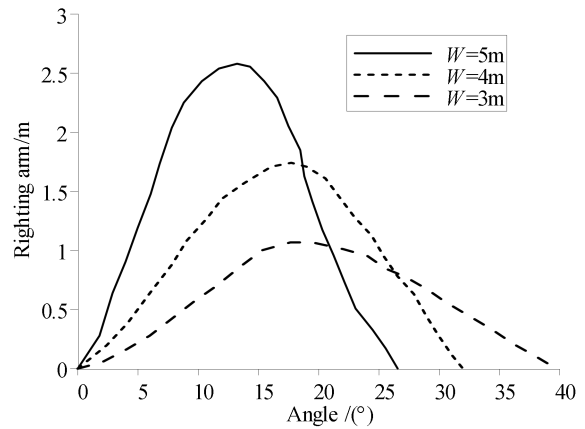


Fig. 13. Stability curves for the different widths

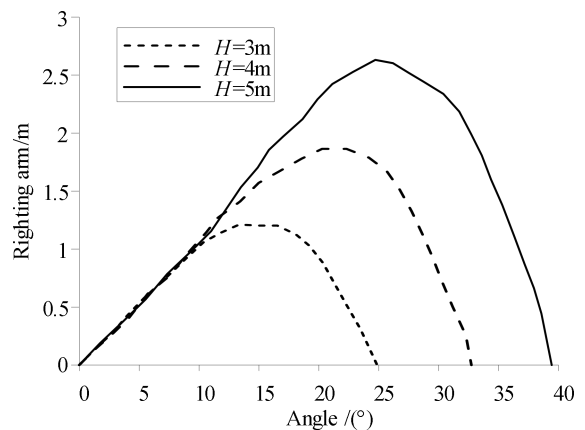


Fig. 14. Stability curves for the different heights

Figs. 12–14 analyze the stability of the towing system with the shape and size of the floating base. In Fig. 12, the maximum righting arm of the floating base, across three distinct shapes, corresponds to an inclined angle of approximately 20°, indicating that the floating robot with varying shapes remains stable under current conditions. Fig. 13 demonstrates that the stability of the towing system continues to increase as the diameter of the floating base becomes larger when other factors are the same. However,

the stability will not continuously increase when the stability increases to a certain extent; instead, it will rapidly decrease. Accordingly, an appropriate allowance should be provided when designing the diameter of the floating base. In Fig. 14, the stability of the towing system with the height of the floating base is studied. The result showed that the maximum righting arm increases with the height of the floating base. When the height of the floating base is 3 m, the maximum value of the righting arm is 1.1 m, with the corresponding inclined angle of 18.5, and the towing system is in a steady state. However, the height of the floating base is not the higher the better. When the height of the floating base is 5 m, the maximum righting arm diminishes to 14.6 m, resulting in an imminent overturning of the towing system.

Although the proposed method may not be suitable for assessing instantaneous stability regarding the lateral overturning, the foregoing results underscore the significance of each influencing factor on the stability of the towing system.

VII. CONCLUSION

This work presents the design of a floating multi-robot coordinated towing system, studies the effect of fluid–structure coupling on the floating robot, and analyzes the various factors influencing the stability to mitigate fluid overturning. The kinematics are first analyzed by using the D–H transformation and the dynamics of rigid body mechanics and hydrodynamic theory. Thereafter, the fluid–structure coupling model is established, and the fluid force on the floating robot is analyzed using Fluent software. The stability of the floating robot is analyzed using the stability theory of ships, and the factors that affect the stability are analyzed. The results indicate that the distinctive shape of the floating base can diminish flow resistance and enhance the stability of the tow system within the fluid environment. The simulated experiment serves as a reference for the practical application of the towing system, while also providing new ideas for the research of offshore towing devices.

REFERENCES

- [1] F. Gao, W. Z. Guo, and Q. Y. Song. “Research and Development of Heavy Manufacturing Equipment at Home and Abroad”, in *Journal of Mechanical Engineering*, vol. 46, no. 19, Mar. 2010, pp. 92-107.
- [2] C. Su, S. H. Zhang and Z. G. Zhao. “Research on Tension Optimization of an Under-constrained Collaborative Towing System with Multi-helicopters in Inverse Dynamics”, in *Scientific Bulletin Series D: Mechanical Engineering*, vol. 82, no. 01, Nov. 2020, pp. 79-92.
- [3] Z. G. Zhao and T. S. Lu. “Simulation on Kinematics and Stability of Multi-Helicopters Hoist System”, in *Journal of system simulation*, vol. 25, no. 04, Aug. 2013, pp. 790-794.
- [4] Z. G. Zhao, Y. L. Wang, and J. H. Li. “Appraise of Dynamical Stability of Multi-robots Cooperatively Towing System Based on Hybrid Force-position-pose Approach”, in *Journal of Harbin Engineering University*, vol. 39, no. 01, Apr. 2018, pp. 148-155.
- [5] J. H. Li, Z. G. Zhao, and S. H. Zhang. “Dynamics and Workspace Analysis of a Multi-robot Collaborative Towing System with Floating Base”, in *Journal of Mechanical Science and Technology*, vol. 35, no. 01, Sep. 2021, pp. 4727-4735.
- [6] X. W. Liu. “3-D Modeling and Force Characteristics of Blue Shark”, in Master’s dissertation, Shanghai Ocean University, 2017.
- [7] M. M. Horoub and M. A. Hawwa. “Influence of Cables Layout on the Dynamic Workspace of a 6-DOF Parallel Marine Manipulator”, in *Mechanism and Machine Theory*, vol. 129, Jul. 2018, pp. 191-201.
- [8] S. Chandrasekaran and A. Jain. “Triangular configuration tension leg platform behavior under random sea wave suspended objects”, in *Ocean Engineering*, vol. 29, no. 15, Dec. 2002, pp. 1895-1928.
- [9] K. Y. Lee, J. H. Cha and K. P. Park. “Dynamic Response of a Floating Crane in Waves by Considering the Nonlinear Effect of Hydrostatic Force”, in *Ship Technology Research*, vol. 5, no. 19, Jan. 2010, pp. 62-71.
- [10] E. Katrin, K. Edwin and M. Marian. “Nonlinear dynamics of floating cranes”, in *Nonlinear Dynamics*, vol. 27, no. 02, Jun. 2002, pp. 107-183
- [11] Yan-qiu Dong and Wei-xue Lin. “Dynamic response of crane boom under wave action”, in *Journal of Tianjin University*, vol. 1, Feb. 1987, pp. 69-76.
- [12] Yan-qiu Dong and Guang Han. “Dynamic response of crane towing system in waves”, in *China Shipbuilding*, vol. 1, Apr. 1993, pp. 63-71.
- [13] Y. F. Mao, K. Q. Zhu, and B. Jing. “Dynamic Response Analysis of Two Floating Cranes System in Irregular Waves”, in *Journal of Waterway and Harbor*, vol. 38, no. 01, Aug. 2017, pp. 31-37.
- [14] C. Zhou, K. Q. Zhu, and Y. F. Mao. “Analysis of the Dynamic Response of the Towing System Under Wave Flow”, in *Waterway and Port*, vol. 39, no. 03, Jun. 2018, pp. 341-347.
- [15] Y. Z. Wang, Y. C. Long and C. Y. Wang. “Simplified Calculation Method of Wave Force of Pile Foundation Considering the Influence of Fluid-solid Coupling”, in *Waterway and Port*, vol. 2, Apr. 2014, pp. 93-98.
- [16] J. Y. Gu, J. M. Yang and H. N. Lv. “Studies of TLP Dynamic Response Under Wind, Waves, and Currents”, in *China Ocean Engineering*, vol. 26, May. 2012, pp. 363-378.
- [17] X. Z. Zhang, W. P. Huang, and H. J. Li. “Nonlinear Dynamic Analysis of Ocean Platform Structure When Considering Fluid-solid Coupling”, in *Journal of the Ocean University of China*, vol. 35, no. 05, Sep. 2005, pp. 823-826.
- [18] Hong-yan Ding, Yan-li Han, and Pu-yang Zhang. “Numerical simulation on floating behavior of buoyancy tank foundation of anemometer tower”, in *Transactions of Tianjin University*, vol. 20, no. 04, Aug. 2014, pp. 243-249
- [19] Y. L. Liu. “Roll Stability Catastrophe Mechanism of a Flooded Ship on Regular Sea Waves”, in *Chinese Physics B*, vol. 23, no. 04, Feb. 2014, pp. 400-403.
- [20] J. W. Zhang, W. W. Wu, and J. Q. Hu. “Quantification of Ship Overturning Under Random Waves”, in *Journal of Dalian Maritime University*, vol. 42, no. 02, May. 2016, pp. 28-34.
- [21] Meng-yao Sun, Yu-hong Liu and Ming-long Huang. “Dynamic stability design of measuring deep water AUV vertical plane”, in *Mechanical Science and Technology*, vol. 35, no. 09, Aug. 2016, pp. 402-1407.
- [22] X. L. Jia and Y. S. Yang. “The Mathematical Model of Ship Motion”, in *Dalian: Dalian Maritime University Press*, 1999.
- [23] R. C. Zhu and G. P. Miao. “Theory of Ship Motion on Waves”, in *Shanghai: Shanghai Jiao Tong University Press*, 2019.
- [24] Y. Q. Zheng, S. N. Jiao, and Y. B. Yang. “Analysis of Dynamic Characteristics of Fluid-solid Coupling Effect of the WDPSS-8 Robot System in a Low-speed Wind Tunnel”, in *Chinese Journal of Mechanical Engineering*, vol. 24, no. 13, Jul. 2013, pp. 1765-1772.
- [25] Z. F. Li and Y. S. Yang. “Simulation of Longitudinal and Sinking Motion of Ships in Regular Waves”, in *Journal of Dalian Maritime University*, no. 04, Dec. 2002, pp. 13-16.

Dongna Li, born in 1981, is an associate professor and teacher at the School of Mechanical Engineering at Lanzhou Jiaotong University. Her primary research focus lies in the field of complex system modeling.